Convective heat transfer optimization in a circular tube based on local exergy destruction minimization

Junbo Wang [a], Zhichun Liu [a], Fang Yuan [a], Wei Liu [a,*], Gang Chen [b]

[a] School of Energy and Power Engineering, Huazhong University of Science and Technology, Wuhan 430074, PR China
[b] State Key Laboratory of Coal Combustion, Huazhong University of Science and Technology, Wuhan 430074, PR China

ABSTRACT

In this study, the equilibrium equation of available potential, which reveals the relation of available potential and local exergy destruction rate, is determined, and the expressions of available potential and local exergy destruction rate are given. To improve heat transfer enhancement and reduce increase amplitude of flow resistance, a method termed as fluid-based heat transfer enhancement is proposed relative to surface-based heat transfer enhancement. An optimal mathematical model by constructing Lagrange function with exergy destruction corresponding to irreversibility loss of heat transfer process and fluid power consumption to flow loss of fluid is adopted to validate this method. To obtain the optimal flow structure in a tube, the tube flow is divided into two parts: core flow and boundary flow. For reducing the irreversibility loss in the core flow, we take fluid exergy destruction as optimization objective with prescribed fluid power consumption. For reducing the flow resistance in the boundary flow, we take fluid power consumption as optimization objective with prescribed fluid exergy destruction. The optimization equations for the convective heat transfer in laminar flow are derived, which are solved numerically. The longitudinal swirling flows in the tube are found at different parameters. In the optimized flow, heat transfer is enhanced greatly while accompanied with a little increase of flow resistance. Comprehensive performance, the ratio of increases in heat transfer and flow resistance, reaches at 3.65 after optimization.

1. Introduction

The enhancement and optimization of heat transfer are essential for energy conservation and environment protection, because heat transfer is related to almost 80% of total energy consumption in industry. Convective heat transfer is one of the common transport processes in industry. It is highly important to develop a theory and corresponding technology for enhancing convective heat transfer.

Through numerical simulation and experimental analysis, researchers have developed many technologies to enhance the heat transfer in tube flow. Correspondingly, certain heat-transfer-enhanced tubes are exploited, such as inner-finned tubes [1], spiral corrugated tubes [2], and micro-finned tubes [3]. Bejan et al. [4] divided the tube flow into two parts: boundary flow and core flow. The flow near the wall of tube is defined as boundary flow and the remaining is core flow. In the aforementioned heat-transfer-enhanced tubes, the surfaces in the boundary, which

dominate the convective heat transfer between fluid and tube wall, are designed or improved to enhance heat transfer. The mechanism for heat transfer enhancement includes [5]: disturbing the boundary layer, extending the heat transfer surface, and changing the physical properties of the heat transfer surface. Therefore, this kind of method can be designated as surface-based heat transfer enhancement (abbreviated as the surface-based method). This method effectively enhances the convective heat transfer coefficient, but the increase in flow resistance may become significant and the comprehensive performance can be weakened.

For reducing the increase in flow resistance while maintaining satisfactory heat transfer, researchers have developed certain new heat-transfer-enhanced tubes, such as center-cleared twisted tape [6], multiple regularly spaced twisted tapes [7], and conical strip inserts [8]. Furthermore, Mohamad and Pavel [9,10] conducted a numerical simulation for heat transfer enhancement in a fully developed tube with porous media partially filling the center. Ming et al. [11] and Huang et al. [12] conducted a brief numerical and experimental study of the heat transfer performance of a tube filled with porous media in the core flow. Wang et al. [13] added fiber fines in a fully developed laminar rectangular channel,

* Corresponding author. Tel.: +86 2787541998; fax: +86 2787540724.
 E-mail address: w_liu@hust.edu.cn (W. Liu).

Nomenclature

A_1, B_1, C_1	Lagrange multipliers
A_2, B_2, C_2	Lagrange multipliers
c_p	specific heat capacity, J/(kg K)
e	available potential, J/kg
e_d	local exergy destruction rate, W/m^3
E_d	exergy destruction, W
f	flow resistance coefficient
F	additional volume force, N/m^3
h	enthalpy, J/kg
J_1, J_2	Lagrange functions
Nu	Nusselt number
p	pressure, Pa
P_w	fluid power consumption, W
$\mathbf{q}$	heat flux, W/m^2
$\mathbf{q}_e$	exergy flux, W/m^2
$\mathbf{q}_s$	entropy flux, W/(m^2 K)
$\dot{q}'''$	inner heat source, W/m^3
$\dot{q}_e'''$	analogical exergy source, W/m^3
$\dot{q}_s'''$	analogical entropy source, W/(m^3 K)
Q	heat, J
s	entropy, J/(kg k)
s_g	local entropy generation rate, W/(m^3 K)
t	time, s

T	temperature, K
U	velocity, m/s
V	volume, m^3

Greek symbols

β	field synergy angle, degree
ε	dimensionless thickness of equivalent thermal boundary layer
λ	heat conductivity, W/(m K)
ρ	fluid density, kg/m^3
μ	viscosity coefficient, kg/(m s)
ϕ	heat dissipation from fluid viscosity, W/m^3
ϕ_e	analogical exergy flow from fluid viscosity, W/m^3
ϕ_s	analogical exergy flow from fluid viscosity, W/(m^3 K)
Ω	fluid computational domain, m^3
Γ	flow boundary area, m^2

Subscripts

0	reference point, environmental state
1	state 1
2	state 2

---

and conducted numerical and experimental studies to characterize the heat transfer and pressure drop. Nanan et al. [14] experimentally investigated heat transfer enhancement through perforated helical twisted tapes and indicated that the use of these tapes reduces friction loss, but yields lower thermal performance factors compared with helical twisted tapes. Tu et al. [15] conducted experimental studies on heat transfer and friction factor characteristics of turbulent flow through a circular tube with small pipe inserts. They found that pipe inserts can transfer more heat at the same pumping power for their unique structure when compared with other inserts, and their performance evaluation criterion (PEC) arrived at 2.23–2.7. These technologies focus on the disturbance in core flow and enhance the heat transfer by changing the tube flow. We designate this method as fluid-based heat transfer enhancement (abbreviated as the fluid-based method). Although this method can achieve satisfactory comprehensive performance, the principle for the design of inserts is not clear. Therefore, it is necessary to develop a theory to reveal the mechanism and an optimization method for the design of inserts.

In addition to the development of techniques for heat transfer enhancement, many related theories have been proposed and developed. Guo et al. [16–18] proposed a new physical quantity called "entransy" to express the capability of the thermal energy transport process. Many modeling and numerical investigations have been conducted; the results have proven that entransy dissipation can be used to express the irreversibility loss when optimizing the heat transfer process. Additionally, Guo et al. [19] proposed the field synergy principle to explain and guide the enhancement of convective heat transfer. Based on Guo's field synergy principle, Liu et al. developed two-field synergy into multi physical quantities synergy, and extended the principle from laminar flow to turbulent flow [20–22]. Based on the principle of multi physical quantities synergy, Liu et al. [23–26] conducted extensive numerical and experimental investigations, which indicated that this theory is an effective method to direct the design of heat transfer processes. Liu et al. [27] also developed a new criterion to evaluate the performance of heat transfer units. Based on entransy, Liu et al. [28] developed a new expression for the second law of thermodynamics and applied it to the optimization of the heat transfer process. Liu

et al. [29] performed numerical investigations to assess the effects of different combinations of entransy and power consumption as optimization objectives or constraint conditions. Additionally, Liu et al. [30] proposed a method for achieving minimum heat consumption to optimize the convective heat transfer, and compared three different objectives, i.e. minimum heat consumption, minimum entransy dissipation, and minimum power consumption. The current methods optimize the convective heat transfer based on the reduction of irreversibility loss, whereas the increase in flow resistance is not taken into consideration. For the operation of a heat exchanger at a constant power consumption by a pump, to reduce the flow resistance means increasing the fluid velocity, thereby achieving better heat transfer performance. Therefore, the reduction of flow resistance is also an effective method to enhance heat transfer. Thus, it is important to simultaneously consider heat transfer enhancement and flow resistance reduction for optimizing the convective heat transfer in a tube.

The concept of exergy is applied widely in analysis and evaluation of energy system and lots of studies have been conducted. Farahat et al. [31] conducted an exergetic optimization of flat plate solar collectors and found the optimal performance and design parameters of these solar to thermal energy conversion systems. Lu et al. [32] established a basic physical model of solar receiver pipe with solar selective coating and conducted exergetic optimization. The variation of energy absorption efficiency and exergetic efficiency with system parameters are analyzed. Bindra et al. [33] conducted thermal analysis and exergy evaluation of packed bed thermal storage systems, and proposed that for packed beds, sensible heat storage systems can provide much higher exergy recovery as compared to phase change material (PCM) storage systems under similar high temperature storage conditions. Furthermore, they [34] developed the sliding flow method to decouple thermal behavior and pressure drop effects and improve the exergetic efficiency. It is significant to analyze the relation between exergy and convective heat transfer.

In this study, we proposed a method, termed fluid-based heat transfer enhancement, for improving the comprehensive performance from the perspective of reducing both thermal and flow resistances. Additionally, we obtained the expression of local

exergy destruction rate based on the analysis of available potential of fluid and constructed a two-objective model to optimize the convective heat transfer.

2. Equilibrium equation of available potential and local exergy destruction rate in heat transfer process

Liu et al. [35] proposed a new variable, designated as available potential, to evaluate the energy grade in fluid with the following expression:

$$e = h - T_0 s, \tag{1}$$

where h is enthalpy, s is entropy, and T_0 is the environmental temperature. Available potential equals total potential h minus unavailable potential $T_0 s$, and depends on the state of fluid.

In heat transfer, available potential changes when the fluid state varies, and the process is expressed as

$$\Delta e = e_1 - e_2 = (h_1 - h_2) - T_0(s_1 - s_2) = \Delta h - T_0 \Delta s, \tag{2}$$

when fluid changes from state 1 to 2, the difference in available potential reflects the transfer of exergy.

Then, the differential equation of Eq. (2) yields

$$\frac{De}{Dt} = \frac{Dh}{Dt} - T_0 \frac{Ds}{Dt}. \tag{3}$$

In heat transfer process, the energy conservation equation of incompressible fluid can be written as follows:

$$\rho \frac{Dh}{Dt} = -\nabla \cdot \boldsymbol{q} + \phi + \dot{q}''', \tag{4}$$

where ρ is the density of fluid and t is the time. The left term of the equation is the change of enthalpy, and the right terms consist of heat fluxes: the first is heat flux from the boundary; the second is heat flux from viscosity dissipation; and the last is heat flux from the inner heat source.

Substituting the relation between entropy and enthalpy, i.e., $Dh = T \cdot Ds$, into Eq. (4), we can obtain the equilibrium equation of entropy for the incompressible fluid:

$$\rho \frac{Ds}{Dt} = -\nabla \cdot \left(\frac{\boldsymbol{q}}{T} \right) + \frac{\lambda(\nabla T)^2}{T^2} + \frac{\phi}{T} + \frac{\dot{q}'''}{T}, \tag{5}$$

that is,

$$\rho \frac{Ds}{Dt} = -\nabla \cdot \boldsymbol{q}_s + s_g + \phi_s + \dot{q}_s'''. \tag{6}$$

The left term in Eq. (6) is the change of entropy in heat transfer. The first one in the right terms is entropy flux transferred with heat flux; the second is the entropy generation rate; the third is analogical entropy flux induced by viscous dissipation; and the last is analogical entropy flux from the inner heat source.

Integrating Eqs. (3)–(5), we have the following equation about available potential:

$$\rho \frac{De}{Dt} = -\nabla \left[\left(1 - \frac{T_0}{T}\right) \boldsymbol{q} \right] - T_0 \frac{\lambda(\nabla T)^2}{T^2} + \left(1 - \frac{T_0}{T}\right) \phi$$
$$+ \left(1 - \frac{T_0}{T}\right) \dot{q}''', \tag{7}$$

that is,

$$\rho \frac{De}{Dt} = -\nabla \cdot \boldsymbol{q}_e - e_d + \phi_e + \dot{q}_e'''. \tag{8}$$

The left term in Eq. (8) is the change of available potential in heat transfer. The first one in the right terms is exergy flux transferred with heat flux from the boundary; the second is the local exergy destruction rate, which reflects the irreversibility loss in heat transfer process; the third is analogical exergy flux induced by viscous dissipation; and the last is analogical exergy flux from the inner heat source.

Eq. (8) reveals the equilibrium relation of available potential. During the heat transfer process, the transfer of exergy induces a change in the fluid state, i.e., available potential. However, due to the irreversibility of the process, there is additional destruction, termed as the local exergy destruction rate. When the exergy flux remains constant, the decrease in the exergy destruction means the achievement of a high available potential state.

Thus far, the equilibrium equation of available potential has been proposed and the expression of local exergy destruction rate is found to measure the irreversibility loss of convective heat transfer.

3. Method of fluid-based heat transfer enhancement

3.1. Description of the method

Many technologies have been developed to enhance the heat transfer in the tube. It is widely known that the enhancement in heat transfer accompanies the increase in flow resistance. As a traditional technique, surface-based heat transfer enhancement concentrates on the extended body on the tube wall, which simultaneously generates a substantial increase of flow resistance in the boundary flow near the tube wall, and may even weaken the comprehensive performance of enhanced heat transfer tube. Thus, to significantly reduce the resistance increase amplitude while maintaining satisfactory heat transfer performance, we introduce a method of fluid-based heat transfer enhancement, which focuses on the fluid disturbance in the core flow in a tube. Many studies have shown that there are plenty of spaces in the core flow region to enhance heat transfer and some corresponding technologies have been reported.

For surface-based heat transfer enhancement, convective heat transfer occurs between the fluid and the heat transfer surface, and the extended surface on the tube wall directly conducts heat from/to the tube. For fluid-based heat transfer enhancement, convective heat transfer only occurs between the fluid and the tube wall, and the disturbance elements or inserts do not conduct heat from/to the tube wall. This implies that there is no heat transfer occurring between the disturbance element surface and the fluid, which is the difference between the two methods.

By inserting a heat transfer unit, the fluid disturbance in core flow alters the flow structure and redistributes the temperature in the core flow region as uniformly as possible. Thus, an equivalent thermal boundary layer with a larger temperature gradient will be formed near the tube wall, which results in significant heat transfer enhancement. Additionally, the bound between the core and boundary flows will become clear in the tube, and the core flow and boundary flow can be coupled to develop a model of heat transfer enhancement.

For a given power consumption, reducing the flow resistance in a process means that heat transfer can be conducted at a higher fluid velocity, which is beneficial to heat transfer enhancement. That is, reducing flow resistance is another method to improve the performance of heat exchangers. Fluid-based method focuses on reducing fluid power consumption. There are several methods which can effectively reduce flow resistance: (1) minimizing the velocity gradient near the tube wall to avoid excessive fluid shear force; (2) minimizing the fluid disturbance in the hydrodynamic region to avoid excessive loss of fluid momentum; (3) minimizing the area of extended surface or insert as far as possible to avoid excessive surface friction. Beyond these, there are other rules for reducing flow resistance: the visual windward area should be

made as small as possible, and the enhanced components should be arranged discretely along the flow direction and so on.

We summarize the characteristics of fluid-based heat transfer enhancement mainly as: (1) no convective heat transfer between the surface of disturbance element and the fluid; (2) formation of an equivalent thermal boundary layer; (3) reduction of flow resistance in the hydrodynamic region of tube. The goals of fluid-based heat transfer enhancement are: (1) to attain a uniform fluid temperature in the core flow while a higher temperature gradient in the boundary flow near the tube wall; (2) to attain a relatively small increase amplitude in flow resistance [36].

3.2. Two-objective model for validating the method

For laminar flow and heat transfer problems, three conservation laws are always the primary principles, which constrain the fluid motion and heat transfer:

(1) Mass conservation law

$$\nabla \cdot \boldsymbol{U} = 0; \tag{9}$$

(2) Momentum conservation law

$$\rho(\boldsymbol{U} \cdot \nabla)\boldsymbol{U} = -\nabla p + \mu\nabla^2\boldsymbol{U} + \boldsymbol{F}; \tag{10}$$

(3) Energy conservation law

$$\lambda\nabla^2 T - \rho c_p \boldsymbol{U} \cdot \nabla T = 0. \tag{11}$$

According to fluid-based method, fluid temperature in core flow region should be distributed as uniformly as possible. Eq. (8) reveals the irreversibility of convective heat transfer with local exergy destruction rate, which represents the unavailable heat loss during the heat transfer process. The minimization of the exergy destruction results in decreased unavailable heat loss. In the flow region, exergy destruction is the integral form of local exergy destruction rate, which can be expressed as

$$E_d = \iiint_\Omega (e_d)dV = \iiint_\Omega \left[T_0 \frac{\lambda(\nabla T)^2}{T^2} \right] dV \tag{12}$$

By analyzing the expression of local exergy destruction rate, it can be found that the smaller the local exergy destruction rate, the smaller the temperature gradient and the higher the fluid temperature in the core flow, which is consistent with the principles of fluid-based method. Therefore, local exergy destruction rate can be taken as the optimization objective for core flow enhancement.

The enhancement of heat transfer is usually accompanied by an increase in flow resistance. To achieve an element of high-performance heat transfer, it is necessary to consider this discrepancy. Liu et al. [27] proposed fluid power consumption by analyzing the synergy based on the conservation equation for mechanical energy, which equals the sum of kinetic energy loss and viscous dissipation work. By making fluid power consumption as small as possible while maintaining a constant heat transfer rate, the optimized flow can be achieved. Total fluid power consumption for incompressible laminar flow is expressed as

$$P_w = \iiint_\Omega [(\rho\boldsymbol{U} \cdot \nabla\boldsymbol{U} - \mu\nabla^2\boldsymbol{U}) \cdot \boldsymbol{U}]dV = \iiint_\Omega [(-\nabla_p) \cdot \boldsymbol{U}]dV \tag{13}$$

Therefore, the mathematical optimal model for fluid-based method can be constructed by using a two-region method; i.e., (1) minimizing exergy destruction with prescribed fluid power consumption in core flow region; (2) minimizing fluid power consumption with prescribed exergy destruction in boundary flow region. Based on the preceding method, the optimal mathematical model can be constructed and the governing equations for the optimized flow field can be achieved by constructing Lagrange function and corresponding variation [29].

In this model, certain boundary conditions should be taken into consideration.

Constant velocity at boundaries, written as variation:

$$\delta\boldsymbol{U}|_\Gamma = 0. \tag{14}$$

Constant viscous shearing stress at boundaries, written as variation:

$$\delta(\mu\nabla\boldsymbol{U})|_\Gamma = \delta(\nabla\boldsymbol{U})|_\Gamma = 0. \tag{15}$$

Constant wall temperature or heat flux at boundaries, written as variation:

$$\delta T|_\Gamma = 0 \quad \text{or} \quad \delta(\lambda\nabla T)|_\Gamma = \delta(\nabla T)|_\Gamma = 0. \tag{16}$$

In core flow (region I), the generalized Lagrange function can be constructed according to the optimization objective and corresponding constraint conditions:

$$J_1 = \iiint_\Omega \left\{ T_0 \frac{\lambda(\nabla T)^2}{T^2} + C_1[\rho(\boldsymbol{U} \cdot \nabla)\boldsymbol{U} - \mu\nabla^2\boldsymbol{U}] \cdot \boldsymbol{U} + A_1\nabla \cdot \boldsymbol{U} \right. $$
$$\left. + B_1(\lambda\nabla^2 T - \rho c_p \boldsymbol{U} \cdot \nabla T) \right\}dV, \tag{17}$$

where C_1, A_1, and B_1 are Lagrange multipliers; C_1 is a constant and A_1 and B_1 are variables.

By using functional variation with respect to velocity, $\boldsymbol{U}$, we can obtain the following optimization equation:

$$\rho C_1 \boldsymbol{U} \cdot \nabla\boldsymbol{U} + \rho C_1 \boldsymbol{U} \times (\nabla \times \boldsymbol{U}) - 2C_1\mu\nabla^2\boldsymbol{U} - \nabla A_1 - \rho c_P B_1 \nabla T = 0. \tag{18}$$

By comparing Eq. (18) with general momentum equation, if allowing

$$\nabla A_1 = -C_1\nabla p + \rho C_1 \boldsymbol{U} \times (\nabla \times \boldsymbol{U}) - C_1\mu\nabla^2\boldsymbol{U}, \tag{19}$$

we can obtain a new momentum equation (a particular solution):

$$\rho(\boldsymbol{U} \cdot \nabla)\boldsymbol{U} = -\nabla p + \mu\nabla^2\boldsymbol{U} + \boldsymbol{F_1}, \tag{20}$$

where the additional volume force, $\boldsymbol{F_1}$, for the optimized flow field is

$$\boldsymbol{F_1} = \frac{\rho c_p B_1 \nabla T}{C_1} \tag{21}$$

By using functional variation with respect to temperature, T, we can obtain the following constraint equation of variable B_1:

$$-\frac{2T_0\lambda\nabla^2 T}{T^2} + \frac{2T_0\lambda(\nabla T)^2}{T^3} + \rho C_P \boldsymbol{U}\nabla B_1 + \lambda\nabla^2 B_1 = 0 \tag{22}$$

and corresponding boundary conditions for the unknown scalar B_1:

$$\left(\frac{2T_0\lambda\nabla T}{T^2} - \rho C_P B_1 \boldsymbol{U} - \lambda\nabla B_1 \right)\delta T + \lambda B_1\delta(\nabla T) = 0. \tag{23}$$

For the boundary condition of constant wall temperature, Eq. (23) can be simplified as

$$B_1 = 0 \tag{24}$$

and the boundary condition of constant heat flux as

$$\frac{2T_0\lambda\nabla T}{T^2} - \lambda\nabla B_1 = 0. \tag{25}$$

For boundary flow region (region II), the generalized Lagrange function can be constructed according to the optimization objective and the corresponding constraint conditions:

$$J_2 = \iiint_{\Omega} \left\{ \boldsymbol{U} \cdot [\rho(U \cdot \nabla)\boldsymbol{U} - \mu\nabla^2 \boldsymbol{U}] + C_2 T_0 \lambda \frac{(\nabla T)^2}{T^2} + A_2 \nabla \cdot \boldsymbol{U} \right.$$
$$\left. + B_2(\lambda\nabla^2 T - \rho C_p \boldsymbol{U} \cdot \nabla T) \right\} dV, \tag{26}$$

where C_2, A_2, and B_2 are Lagrange multipliers; C_2 is a constant and A_2 and B_2 are variables.

By using functional variation with respect to velocity, $\boldsymbol{U}$, we can obtain the following optimization equation:

$$\rho\boldsymbol{U} \cdot \nabla\boldsymbol{U} + \rho\boldsymbol{U} \times (\nabla \times \boldsymbol{U}) - 2\mu\nabla^2\boldsymbol{U} - \nabla A_2 - \rho c_P B_2 \nabla T = 0. \tag{27}$$

By comparing Eq. (27) with common momentum equation, if allowing

$$\nabla A_2 = -\nabla p + \rho\boldsymbol{U} \times (\nabla \times \boldsymbol{U}) - \mu\nabla^2\boldsymbol{U}, \tag{28}$$

we can obtain a new momentum equation (a particular solution):

$$\rho(\boldsymbol{U} \cdot \nabla)\boldsymbol{U} = -\nabla p + \mu\nabla^2\boldsymbol{U} + \boldsymbol{F_2}, \tag{29}$$

where the additional volume force, $\boldsymbol{F_2}$, for the optimized flow field is

$$\boldsymbol{F_2} = \rho c_p B_2 \nabla T. \tag{30}$$

By using functional variation with respect to temperature, T, we can obtain the following constraint equation of variable B_2:

$$-\frac{2C_2 T_0 \lambda\nabla^2 T}{T^2} + \frac{2C_2 T_0 \lambda(\nabla T)^2}{T^3} + \rho c_P \boldsymbol{U}\nabla B_2 + \lambda\nabla^2 B_2 = 0 \tag{31}$$

and corresponding boundary conditions for unknown scalar B_2:

$$\left(\frac{2C_2 T_0 \lambda\nabla T}{T^2} - \rho C_P B_2 \boldsymbol{U} - \lambda\nabla B_2 \right)\delta T + \lambda B_2 \delta(\nabla T) = 0. \tag{32}$$

For the boundary condition of constant wall temperature, Eq. (32) can be simplified as

$$B_2 = 0 \tag{33}$$

and the boundary condition of constant heat flux as

$$\frac{2C_2 T_0 \lambda\nabla T}{T^2} - \lambda\nabla B_2 = 0. \tag{34}$$

Through variations on Lagrange functions in core and boundary regions, the governing equations for optimal flow in the flow region can be expressed as

$$\begin{cases} \rho(\boldsymbol{U} \cdot \nabla)\boldsymbol{U} = -\nabla p + \mu\nabla^2\boldsymbol{U} + \boldsymbol{F}, \\ \nabla \cdot \boldsymbol{U} = 0, \\ \lambda\nabla^2 T - \rho C_p \boldsymbol{U} \cdot \nabla T = 0. \end{cases} \tag{35}$$

When fluid flows in core region, the additional volume force $\boldsymbol{F}$ in Eq. (35) is $\boldsymbol{F_1}$, which is related to B_1 in Eq. (21) and its constraining equation, Eq. (22); when fluid flows in boundary region, $\boldsymbol{F}$ becomes $\boldsymbol{F_2}$, which is related to B_2 in Eq. (30) and its constraining equation, Eq. (31).

Mathematical optimal model has been constructed by minimizing different objectives in core and boundary flows. The governing equations for the flow with the best comprehensive performances of heat transfer and flow are obtained as Eq. (35). By solving the governing equations, the optimized flow and temperature fields optimized by fluid-based method can be achieved.

4. Numerical verification of laminar flow in a tube

The fluid-based heat transfer enhancement takes both of heat transfer performance and flow characteristic into consideration. To validate this method, the optimized governing equation (35) deduced from the model is solved by numerical calculation.

The Prandtl number of water is intermediate, which means that flow and thermal boundary layers can achieve full development at
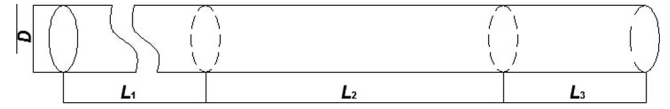
Fig. 1. Schematic of calculation model.

a close length. Furthermore, water is commonly used in heat exchanger, so it is chosen as the working fluid in this calculation.

The schematic of the calculation model is shown in Fig. 1, for which the detailed parameters are as follows: a circular tube with dimensions $D = 20$ mm, $L_1 = 1200$ mm, $L_2 = 300$ mm, and $L_3 = 200$ mm, where D is the tube diameter, L_1 is the length of entrance region, L_2 is calculation domain of heat transfer optimization, and L_3 is the length of stable region. Thus, water flows with an inlet Reynolds number and achieves full development at the end of entrance region, then the additional force affects the flow in the calculation region to achieve the optimal result.

The inlet temperature and Reynolds number are 300 K and 200. The tube walls of entrance and calculation regions are maintained at a constant temperature of 310 K. The wall of the stable region is adiabatic in this calculation.

The governing equation for the calculation region is Eq. (35). By solving the governing equations, we can determine the optimal flow structure and temperature field. The commercial computational fluid dynamics (CFD) software FLUENT 6.3 is adopted in this calculation. The SIMPLEC algorithm is used for pressure–velocity coupling; the QUICK scheme is adopted to discretize convection and diffusion terms. The user defined function (UDF) and user defined scalar (UDS) are utilized to solve the unknown parameters and volume forces. The convergent solutions are obtained when the residuals are less than 10^{-5}.

Grid independent test has been performed for the physical model. Hexahedral grid is adopted in this calculation and the grid of boundary layer is refined. Three grid systems with 1,780,818, 3,059,392 and 5,918,747 cells are adopted to calculate a baseline case. From the calculated values obtained by the three grid systems, the 3,059,392-grid system with 1.4% deviation of Nusselt number, is found to be dense enough to result in the grid independent solutions. To validate the accuracy of the numerical solutions, the Nusselt number (Nu) and the friction factor (f) of bare tube are calculated and compared with theoretical values (3.66 and 64/Re) when the Reynolds number (Re) is 200. The deviation of Nu and f are less than 2%.

When the flow achieves full development, the boundary layer meets at the center of a tube. According to the principles of fluid-based method, we hope to form an equivalent thermal boundary layer. In the calculation, therefore, we need to determine the thickness of equivalent thermal boundary artificially and search for the optimal value. The entire flow region in the tube is separated into the core and boundary flow regions. The former is a circular region with diameter D_1, and the latter is an annular region, as shown in Fig. 2. The dimensionless thickness can be defined as
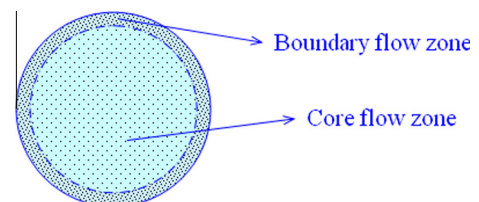
Fig. 2. Division of calculation regions.

Table 1
Performance with different dimensionless thickness ($C_1 = -1 \times 10^6$, $C_2 = -3 \times 10^{-7}$, $P_w = 8.34 \times 10^{-7}$ W, $Re = 200$).

ε	Nu/Nu_0	f/f_0	$(Nu/Nu_0)/(f/f_0)$
0.05	3.48	1.18	2.95
0.1	3.35	1.10	3.05
0.2	3.1	1.06	2.92
0.3	2.46	1.05	2.34

$$\varepsilon = \frac{D - D_1}{D}. \tag{36}$$

Calculation was conducted to determine a relatively optimal value of dimensionless thickness and the data was shown in Table 1. Nu_0 and f_0 are the Nusselt number and friction resistance coefficient of bare tubes. The value of $(Nu/Nu_0)/(f/f_0)$ is used to evaluate the comprehensive performance by simultaneously considering the heat transfer enhancement and flow resistance increase. When dimensionless thickness decreases, both of Nu and f increase, while comprehensive performance increases first and then decreases. The case with 0.1 has the best comprehensive performance among cases calculated, and dimensionless thickness is chosen as 0.1 in this study (see Table 2).

Two parameters, C_1 and C_2, can be adjusted to change the fluid power consumption condition. By solving the governing equations, the optimal flow form is obtained under prescribe power consumption. Moreover, optimal flows under different power consumptions are shown in Figs. 3–6. From Figs. 3–6, the flow form is a longitudinal swirl flow with multi-vortexes under different combinations of C_1 and C_2. That means longitudinal swirl flow is an optimal flow under certain power consumption. Besides, there are a few differences between the optimal flows under different power consumptions. There is a vortex strip in the core flow region, which consists of eight vortexes, as shown in Fig. 3. These vortexes disturb the core flow, thus changing the temperature field. The temperature in the core flow region is distributed uniformly. Simultaneously, an equivalent thermal boundary layer is formed in the boundary flow region. When C_1 keeps constant but C_2 changes, 12 vortexes are generated, as shown in Fig. 4. In addition, the vortex strip is smaller and closer to the wall than that in Fig. 3. Accordingly, the equivalent thermal layer becomes thinner and the temperature gradient near the tube wall higher. By changing the combination of C_1 and C_2, flow structure and temperature field are changed. As shown in Fig. 5, the temperature field and flow structure are similar to those shown in Fig. 4, but certain vortexes in the vortex strip become large. In Fig. 6, the vortex strip consists of alternated large and small vortexes. The large vortexes disturb the core flow so that the temperature is distributed more uniformly. The small vortexes make equivalent thermal boundary layer thinner and temperature gradient near the tube wall higher. By comparing the temperature field in Fig. 6 with that in Figs. 3–5, the temperature in the core flow region, which occupies large parts of flow region, is distributed uniformly and remains high. The outer region is boundary flow with high temperature gradient.

For the model of a tube, optimal governing equation (35) was numerically solved. Moreover in cases of different power

Table 2
Comparison between optimized and bare tubes in different fields.

C_1	C_2	$P_w \times 10^7$ (W)	Nu/Nu_0	f/f_0	U_r/U_m (%)	$(Nu/Nu_0)/(f/f_0)$
-1×10^6	-3×10^{-7}	8.34	3.35	1.10	1.58	3.05
-1×10^6	-1×10^{-5}	10.9	4.85	1.43	5.75	3.39
-4×10^7	-1×10^{-5}	11.9	5.53	1.56	9.66	3.54
-4×10^7	-2×10^{-5}	15.3	7.20	1.97	16.90	3.65
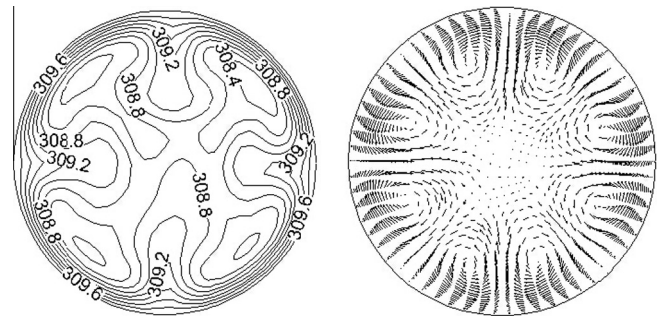
Fig. 3. Temperature and flow field at $L = 1350$ mm ($C_1 = -1 \times 10^6$, $C_2 = -3 \times 10^{-7}$, $P_w = 8.34 \times 10^{-7}$ W, $Re = 200$).
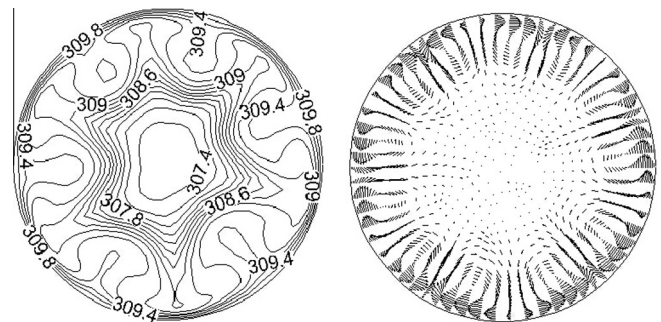
Fig. 4. Temperature and flow field at $L = 1250$ mm ($C_1 = -1 \times 10^6$, $C_2 = -1 \times 10^{-5}$, $P_w = 1.09 \times 10^{-6}$ W, $Re = 200$).
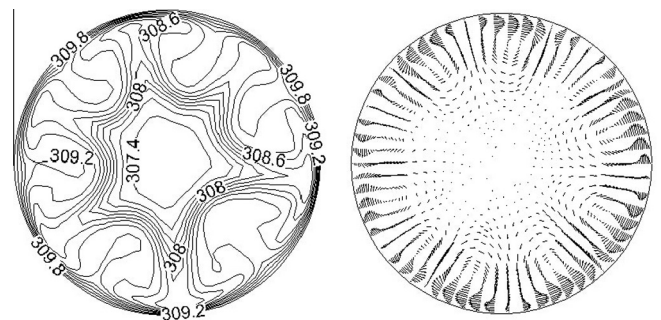
Fig. 5. Temperature and flow field at $L = 1250$ mm ($C_1 = -4 \times 10^7$, $C_2 = -1 \times 10^{-5}$, $P_w = 1.19 \times 10^{-6}$ W, $Re = 200$).
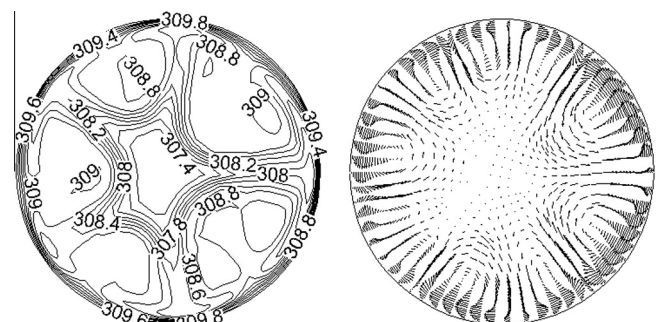
Fig. 6. Temperature and flow field at $L = 1250$ mm ($C_1 = -4 \times 10^7$, $C_2 = -2 \times 10^{-5}$, $P_w = 1.53 \times 10^{-6}$ W, $Re = 200$).

consumption, the optimal flow forms are all longitudinal swirl flows with multi-vortexes, as shown in Figs. 3–6. In momentum equation, the additional force is determined by temperature field,
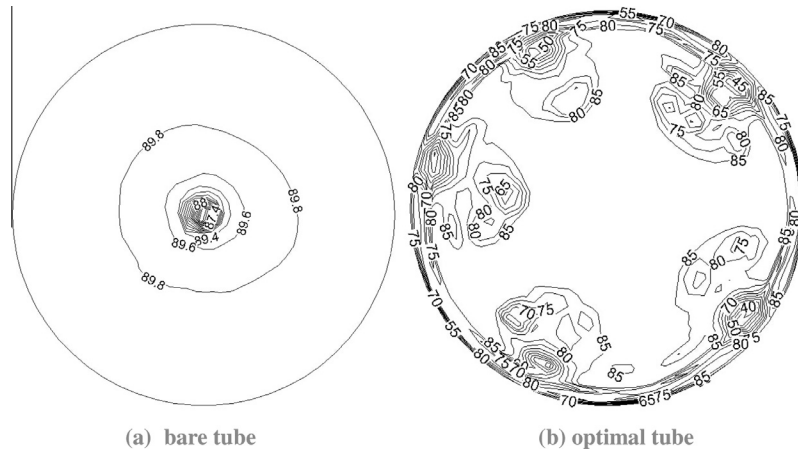
Fig. 7. Distribution of field synergy angle β at $L = 1250$ mm ($C_1 = -4 \times 10^7$, $C_2 = -2 \times 10^{-5}$, $P_w = 1.53 \times 10^{-6}$ W, $Re = 200$).

and the force improves the synergy of velocity and temperature fields. Fig. 7 show the distribution of synergy angle β which is proposed to evaluate heat transfer enhancement in Ref. [19]. The vortexes greatly improve the synergy of velocity and temperature fields, and the average β of calculation region is reduced from 89.8° to 84.7°.

Fig. 8 shows the flow structure in the calculation domain. At the end of the entrance region, the flow achieves full development, and a longitudinal swirling flow appears in the flow region under the effect of additional volume force. By considering Figs. 6 and 8, we can draw the conclusion that longitudinal swirling flow with multi-vortexes is the optimal flow pattern.

To more clearly observe the temperature field, temperature variations of bare and optimized tubes in the radial direction are presented in Fig. 9. As shown in Fig. 9, the temperature variation of bare tube is parabolic and far from the ideal temperature distribution. The vortexes distribute the temperature uniformly in the core flow, as shown in Fig. 9. Accordingly, an equivalent boundary layer is formed near the tube wall. When the vortex form changes, the temperature distribution varies correspondingly. There is a region in the core flow which has a relatively high temperature, which makes the temperature gradient in the boundary flow increased. Additionally, the region of low temperature lessens with the increase of disturbance intensity (more fluid power consumption). Uniform distribution of temperature in the core flow and formation of an equivalent thermal boundary layer are the reasons for the enhancement of heat transfer.

To verify the method of fluid-based heat transfer enhancement and investigate the heat transfer and flow resistance performance of the optimized flow field, Table 3 provides a comparison of heat transfer and resistance coefficients between optimized and bare tubes under different parameters. The optimized flow structure in our investigation is the longitudinal swirling flow, and the maximal value of $(Nu/Nu_0)/(f/f_0)$ can reaches at 3.65. The ratio of
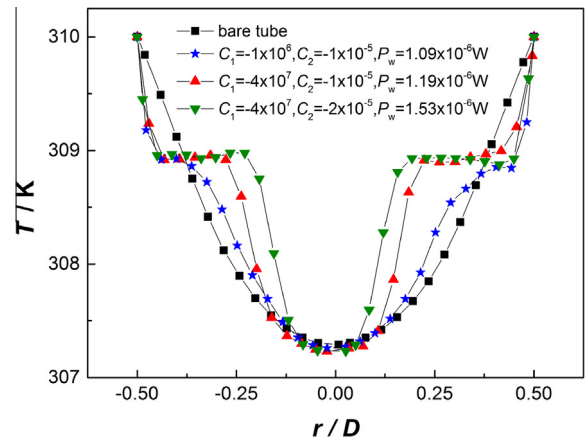
Fig. 9. Temperature variations of bare and optimized tubes in radial direction.

Table 3
Comparison among different optimization methods.

Methods	$P_w \times 10^7$ (W)	Nu/Nu_0	f/f_0	$(Nu/Nu_0)/(f/f_0)$
Exergy destruction	8.45	3.66	1.12	3.27
Entropy generation	8.59	3.60	1.14	3.16
Entransy dissipation [34]	8.39	2.27	1.10	2.06

velocity in the radial direction and main flow direction, U_r/U_m, is less than 17%. Therefore, the increase of flow resistance is weaker than enhancement of heat transfer, which indicates that the flow structure with longitudinal swirling has excellent overall heat transfer performance. In addition, under different conditions, the comprehensive performance is larger than 3. Thus, it indicates that
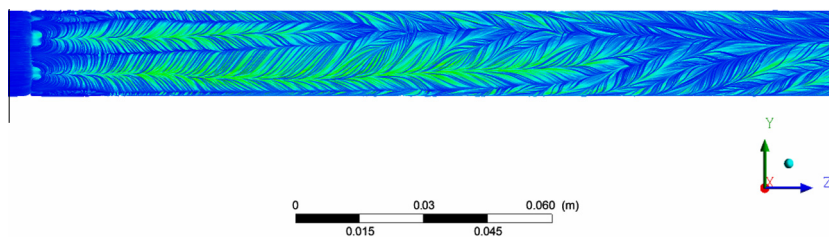
Fig. 8. Longitudinal swirling flow in calculation domain ($C_1 = -4 \times 10^7$, $C_2 = -2 \times 10^{-5}$, $P_w = 1.53 \times 10^{-6}$ W, $Re = 200$).
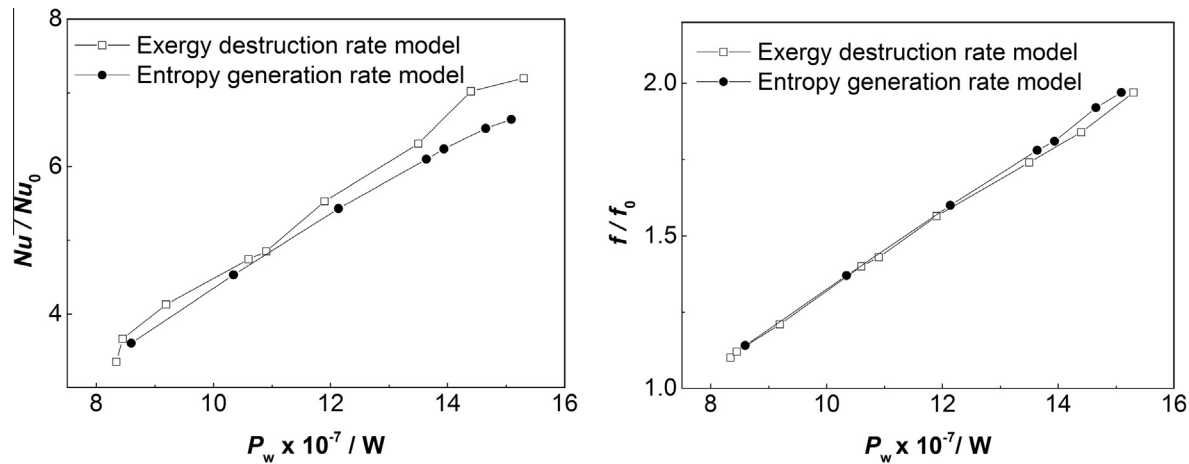
Fig. 10. Comparison of heat transfer and flow resistance performances. between exergy destruction rate model and entropy generation rate model.

the method of fluid-based heat transfer enhancement can be applied in the optimization of convective heat transfer.

In this optimal mathematical model of fluid-based heat transfer enhancement, irreversibility loss is expressed as local exergy destruction rate. From Eq. (10), the local entropy generation rate can also express the irreversibility loss in heat transfer process. Then, another model can be constructed with local entropy generation rate as irreversibility loss. These two models can be designated as exergy destruction rate model and entropy generation rate model, respectively. In addition, through function variation and numerical calculation, a similar optimal temperature field and flow structure can be obtained. Furthermore, a comparison between the two models is conducted. Fig. 10 compares heat transfer and flow resistance performances for these two models. The results show that, for prescribe fluid power consumption, the heat transfer in the exergy destruction rate model is slightly higher than that in the entropy generation rate model, with almost the same flow resistances increase. It indicates that both exergy destruction rate and entropy generation rate can express the irreversibility of the heat transfer process, but exergy destruction rate is more suitable than entropy generation rate to express irreversibility loss because of its specific physical meaning and same unit with energy.

In Ref. [37], Jia et al. proposed an optimization method based on minimum entransy dissipation in circular tube. Entransy dissipation is set as optimization objective in the entire flow region, while fluid power consumption is not taken into consideration. Table 3 shows the comparison among exergy destruction, entropy generation and entransy dissipation models. From the comparison, it indicates that the method in this paper can bring a better comprehensive performance than that in Ref. [37].

By analyzing the performance of convective heat transfer and flow resistance in the optimized tube, the method of fluid-based heat transfer enhancement is demonstrated to be effective. Under different power consumptions, optimal flows are all longitudinal swirling flow with multi-vortexes, which has high heat transfer efficiency and relatively low flow resistance. Furthermore, more fluid power consumption means stronger disturbance and better comprehensive performance.

5. Conclusions

The equilibrium equation of available potential is obtained, in which the local exergy destruction rate is defined to express the irreversibility loss of the convective heat transfer process. Different from the surface-based heat transfer enhancement

method, the fluid-based method is put forward by considering both thermal and flow resistances. The optimal mathematical model is constructed by the two-region method to reflect the principle of fluid-based heat transfer enhancement. By numerically solving the governing equation deduced through functional variation for Lagrange function, the optimal velocity field is obtained. The theoretical analysis is benefit to the high-efficiency and low-resistance heat transfer enhancement technologies. Specific conclusions are summarized as follows.

(1) Available potential represents the energy grade of the fluid, and its equilibrium equation expresses the transport process of available energy. By reducing the exergy destruction of the fluid, the irreversibility of transport process can be decreased.

(2) An optimization method of convective heat transfer is constructed by setting exergy destruction rate as optimization objective in the core flow and fluid power consumption as optimization objective in the boundary flow in a circular tube, which supports the principle of fluid-based heat transfer enhancement.

(3) Numerical results by solving the governing equations show that the optimized flow field in a circular tube is in a structure of longitudinal swirling flows, which shows alternating large and small vortexes in the cross section of tube, and heat transfer can be greatly enhanced with a slight increase in flow resistance.

Conflict of interest

None declared.

Acknowledgments

References

[1] F. Giampietro, Heat transfer optimization in internally finned tubes under laminar flow conditions, Int. J. Heat Mass Transfer 41 (1998) 1243–1253.
[2] P.G. Vicente, A. Garcia, A. Viedma, Experimental investigation on heat transfer and frictional characteristics of spirally corrugated tubes in turbulent flow at different Prandtl numbers, Int. J. Heat Mass Transfer 47 (4) (2004) 671–681.
[3] M. Siddique, M. Alhazmy, Experimental study of turbulent single-phase flow and heat transfer inside a micro-finned tube, Int. J. Refrig. 31 (2008) 234–241.
[4] A. Bejan, A.D. Kraus, Heat Transfer Handbook, John Wiley & Sons, New Jersey, 2003.

[5] R.L. Webb, Principles of Enhanced Heat Transfer, John Wiley, New York, 1994.
[6] J. Guo, A.W. Fan, X.Y. Zhang, W. Liu, A numerical study on heat transfer and friction factor characteristics of laminar flow in a circular tube fitted with center-cleared twisted tape, Int. J. Therm. Sci. 50 (2011) 1263–1270.
[7] X.Y. Zhang, Z.C. Liu, W. Liu, Numerical studies on heat transfer and flow characteristics for laminar flow in a tube with multiple regularly spaced twisted tapes, Int. J. Therm. Sci. 58 (2012) 157–167.
[8] A.W. Fan, J.J. Deng, J. Guo, W. Liu, A numerical study on thermo-hydraulic characteristics of turbulent flow in a circular tube fitted with conical strip inserts, Appl. Therm. Eng. 31 (2011) 2819–2828.
[9] A.A. Mohamad, Heat transfer enhancements in heat exchangers fitted with porous media. Part I: constant wall temperature, Int. J. Therm. Sci. 42 (4) (2003) 385–395.
[10] B.I. Pavel, A.A. Mohamad, An experimental and numerical study on heat transfer enhancement for gas heat exchangers fitted with porous media, Int. J. Heat Mass Transfer 47 (23) (2004) 4939–4952.
[11] T.Z. Ming, Y. Zheng, J. Liu, C. Liu, W. Liu, S.Y. Huang, Heat transfer enhancement by filling metal porous medium in central area of tubes, J. Energy Inst. 83 (1) (2010) 17–24.
[12] Z.F. Huang, A. Nakayama, K. Yang, C. Yang, W. Liu, Enhancing heat transfer in the core flow by using porous medium insert in a tube, Int. J. Heat Mass Transfer 53 (2010) 1164–1174.
[13] S. Wang, Z.Y. Guo, Z.X. Li, Heat transfer enhancements by using metallic filament insert in channel flow, Int. J. Heat Mass Transfer 44 (7) (2001) 1373–1378.
[14] K. Nanan, C. Thianpong, P. Promvonge, S. Eiamsa-ard, Investigation of heat transfer enhancement by perforated helical twisted-tapes, Int. Commun. Heat Mass 52 (2014) 106–112.
[15] W.B. Tu, Y. Tang, B. Zhou, L.S. Lu, Experimental studies on heat transfer and friction factor characteristics of turbulent flow through a circular tube with small pipe inserts, Int. Commun. Heat Mass 56 (2014) 1–7.
[16] Z.Y. Guo, H.Y. Zhu, X.G. Liang, Entransy – a physical quantity describing heat transfer ability, Int. J. Heat Mass Transfer 50 (2007) 2545–2556.
[17] Z.Y. Guo, X.B. Liu, W.Q. Tao, R.K. Shah, Effectiveness – thermal resistance method for heat exchanger design and analysis, Int. J. Heat Mass Transfer 53 (2010) 2877–2884.
[18] Q. Chen, J.X. Ren, Z.Y. Guo, Field synergy analysis and optimization of decontamination ventilation designs, Int. J. Heat Mass Transfer 51 (2008) 873–881.
[19] Z.Y. Guo, W.Q. Tao, R.K. Shah, The field synergy (coordination) principle and its applications in enhancing single phase convective heat transfer, Int. J. Heat Mass Transfer 48 (2005) 1797–1807.
[20] W. Liu, Z.C. Liu, Z.Y. Guo, Physical quantity synergy in laminar flow field of convective heat transfer and analysis of heat transfer enhancement, Chin. Sci. Bull. 54 (2009) 3579–3586.
[21] W. Liu, Z.C. Liu, T.Z. Ming, Z.Y. Guo, Physical quantity synergy in laminar flow field and its application in heat transfer enhancement, Int. J. Heat Mass Transfer 52 (2009) 4669–4672.
[22] W. Liu, Z.C. Liu, Y.S. Wang, S.Y. Huang, Flow mechanism and heat transfer enhancement in longitudinal-flow tube bundle of shell-and-tube heat exchanger, Sci. China Ser. E 52 (2009) 2952–2959.
[23] C. Yang, A. Nakayama, W. Liu, Heat transfer performance assessment for forced convection in a tube partially filled with a porous medium, Int. J. Therm. Sci. 54 (2012) 98–108.
[24] X.Y. Zhang, Z.C. Liu, W. Liu, Numerical studies on heat transfer and friction factor characteristics of a tube fitted with helical screw-tape without core-rod inserts, Int. J. Heat Mass Transfer 60 (2013) 490–498.
[25] J. Guo, Y.X. Yan, W. Liu, F.M. Jiang, A.W. Fan, Effects of upwind area of tube inserts on heat transfer and flow resistance characteristics of turbulent flow, Exp. Therm. Fluid Sci. 48 (2013) 147–155.
[26] Y.S. Wang, Z.C. Liu, S.Y. Huang, W. Liu, W.W. Li, Experimental investigation of shell-and-tube heat exchanger with a new type of baffles, Heat Mass Transfer 47 (2011) 833–839.
[27] W. Liu, Z.C. Liu, L. Ma, Application of a multi-field synergy principle in the performance evaluation of convective heat transfer enhancement in a tube, Chin. Sci. Bull. 57 (2012) 1600–1607.
[28] W. Liu, Z.C. Liu, H. Jia, A.W. Fan, A. Nakayama, Entransy expression of the second law of thermodynamics and its application to optimization in heat transfer process, Int. J. Heat Mass Transfer 54 (2011) 3049–3059.
[29] H. Jia, W. Liu, Z.C. Liu, Enhancing convective heat transfer based on minimum power consumption principle, Chem. Eng. Sci. 69 (2012) 225–230.
[30] W. Liu, H. Jia, Z.C. Liu, H.S. Fang, K. Yang, The approach of minimum heat consumption and its applications in convective heat transfer optimization, Int. J. Heat Mass Transfer 57 (2013) 389–396.
[31] J. Lu, J. Ding, J. Yang, Heat transfer performance and exergetic optimization for solar receiver pipe, Renewable Energy 35 (2010) 1477–1483.
[32] S. Farahat, F. Sarhaddi, H. Ajam, Exergetic optimization of flat plate solar collectors, Renewable Energy 34 (2009) 1169–1174.
[33] H. Bindra, P. Bueno, J.F. Morris, R. Shinnar, Thermal analysis and exergy evaluation of packed bed thermal storage systems, Appl. Therm. Eng. 52 (2013) 255–263.
[34] H. Bindra, P. Bueno, J.F. Morris, Sliding flow method for exergetically efficient packed bed thermal storage, Appl. Therm. Eng. 64 (2014) 201–208.
[35] W. Liu, K. Yang, A. Nakayama, Enhancing heat transfer in the core flow by forming an equivalent thermal boundary layer in the fully developed tube flow, in: Sixth Int. Conf. on Enhanced, Compact and Ultra-compact Heat Exchangers: Science, Engineering and Technology, Potsdam, Germany, 2007.
[36] W. Liu, K. Yang, Mechanism and numerical analysis for heat transfer enhancement in the core flow along a tube, Sci. China Ser. E 51 (8) (2008) 1195–1202.
[37] H. Jia, Z.C. Liu, W. Liu, A. Nakayama, Convective heat transfer optimization based on minimum entransy dissipation in the circular tube, Int. J. Heat Mass Transfer 73 (2014) 124–129.